

Thermo-responsive polyurethane hydrogels based on poly(ethylene glycol) and poly(caprolactone): Physico-chemical and mechanical properties

Lucas Polo Fonseca, Rafael Bergamo Trinca, Maria Isabel Felisberti

Institute of Chemistry, University of Campinas (UNICAMP), P.O. Box 6154, 13083-970 Campinas, SP, Brazil

Correspondence to: M. I. Felisberti (E-mail: misabel@iqm.unicamp.br)

ABSTRACT: In this work, we present the synthesis and characterization of chemically crosslinked polyurethanes (PU) composed of poly(ethylene glycol) (PEG) and poly(caprolactone) diol (PCL-diol), as hydrophilic and hydrophobic segments respectively, poly(caprolactone) triol (PCL-triol), to induce hydrolysable crosslinks, and hexamethylene diisocyanate (HDI). The syntheses were performed at 45 °C, resulting in polyurethanes with different PEG/PCL-diol/PCL-triol mass fractions. All the PUs are able to crystallize and their thermal properties depend on the global composition. The water uptake capacities of the PU increase as the PEG amount increases. The water into hydrogels is present in different environments, as bounded, bulk and free water. The PU hydrogels are thermo-responsive, presenting a negative dependence of the water uptake with the temperature for PEG rich networks, which gradually changes to a positive behavior as the amount of poly(caprolactone) (PCL) segments increases. However, the water uptake capacity changes continuously without an abrupt transition. Scanning electron microscopy (SEM) analyses of the hydrogel morphology after lyophilization revealed a porous structure. Mechanical compression tests revealed that the hydrogels present good resilience and low recovery hysteresis when they are subject to cycles of compression–decompression. In addition, the mechanical properties of the hydrogels varies with the composition and crosslinking density, and therefore with the water uptake capacity. The PU properties can be tuned to fit for different applications, such as biomedical applications. © 2016 Wiley Periodicals, Inc. *J. Appl. Polym. Sci.* **2016**, *133*, 43573.

KEYWORDS: mechanical properties; morphology; polyurethanes; swelling; thermal properties

Received 6 January 2016; accepted 23 February 2016

DOI: 10.1002/app.43573

INTRODUCTION

Polymeric hydrogels are tridimensional polymeric networks, capable of absorbing a high amount of water. Due to their water uptake capacity, potential amphiphilic behavior, and biocompatibility or biodegradability, hydrogels have been intensively studied for applications in the biomedical, pharmaceutical, agriculture, oil recovery, and cosmetics fields as well as in the biotechnology, bioseparation processes, and as biosensors.^{1,2}

Among the different classes of hydrogels, polyurethane hydrogels have raised interest because their properties can be easily modulated by the composition for a wide range of applications.^{3,4} Their good mechanical properties come from the alternation between soft segments, usually polyethers or polyesters, and hard segments composed of the urethane linkages originating from the reaction between isocyanates and hydroxyl end groups of polyols.⁵ The soft segments provide elasticity to the

polymer, while the hard segments provide strength due to the hydrogen bonding between the urethane linkages. These properties are essential in tissue engineering, when aiming for a polymer with mechanical properties similar to the tissue to be repaired. However, they are not usually found in physically crosslinked hydrogels, either in natural polymers such as chitosan and collagen.^{3,4,6}

Biodegradability and biocompatibility are expected and reported for polyurethanes (PU) composed of biocompatible and biodegradable segments such as poly(ethylene glycol) (PEG) and poly(caprolactone) (PCL), respectively.^{7–12} While aromatic diisocyanates in PU generate toxic metabolites *in vivo*, as aromatic amines, the use of aliphatic isocyanates, such as hexamethylene diisocyanate (HDI), is preferential to achieve biocompatibility in polyurethanes.³ Also, the use of aliphatic soft isocyanates can lead to semicrystalline PU.¹³ Polyurethane biodegradability can be modulated by the choice of hydrolysable segments, molar ratio of the precursors, crosslinking density, amphiphilic

Additional Supporting Information may be found in the online version of this article.

© 2016 Wiley Periodicals, Inc.

balance, and crystallinity degree of the polymeric matrix. The presence of a crystalline phase reduces the hydrolytic degradation rate because its dense packing diminishes the water uptake and water–polymer chains interface.^{3,14,15}

Thermo-responsive behavior can be achieved in PUs by copolymerization or blending with thermo-sensitive polymers such as poly(N-isopropylacrylamide) P(NiPAAm)^{16,17} or by adjusting the hydrophilic–hydrophobic balance alternating PEG with aliphatic isocyanates such as HDI or other hydrophobic precursors such as PCL and poly(L-Lactide) (PLLA).¹⁸ By alternating hydrophilic PEG and hydrophobic segments, auto-organized structures are formed as a consequence of micellization or sol–gel transitions in aqueous media, which is of great interest for biomedical applications.^{19–21} Sardon *et al.*²² reported a series of non-crosslinked polyurethane copolymers composed of PEG as hydrophilic segment, isophorene diisocyanate as hydrophobic aliphatic isocyanate, and 2,2-bis(hydroxymethyl)propionic acid as chain extensor. The PU water solutions showed lower critical solution temperature (LCST) behavior with critical temperature dependent on the PEG molar ratio, leading to the formation of physically crosslinked hydrogels.

Chemically crosslinked polyurethane hydrogels properties can be easily modulated by the composition in order to achieve desirable properties such as suitable mechanical properties for biomedical applications.^{23,24} París *et al.*²³ reported the synthesis and the characterization of chemically crosslinked polyurethanes composed of low molar mass PEG ($M_n = 600$ g/mol and 1500 g/mol) and poly(caprolactone) diol (PCL-diol, $M_n = 530$ g/mol) as hydrophilic and hydrophobic segments, respectively, PEG-triol and PEG-tetraol as crosslinking agents, and HDI as isocyanate (NCO/OH molar ratio = 1.05/1). All the reactants were mixed, and the polymerization was conducted in the absence of air. The resulting PUs, containing up to 15 wt % of PCL-diol, were used to prepare hydrogels that, in general, were thermo-responsive, amorphous, and presented good mechanical properties. However, the PU did not present a significant degradation due to the low accessibility of water to the hydrophobic polyester sites and to the non-hydrolysable nature of the crosslinks.

The replacement of non-hydrolysable crosslinks to hydrolysable ones improves the PU degradation rate. In this way, Barrioni *et al.*¹¹ reported the synthesis of chemically crosslinked polyurethanes based on HDI as diisocyanate, low molar mass PEG ($M_n = 600$ g/mol) and glycerol and poly(caprolactone) triol (PCL-triol, $M_n = 900$ g/mol) as hydrolysable crosslinking agents, in order to produce biodegradable polyurethane films by the pre-polymer process. The PCL-triol amount in the two synthesized polyurethanes was 3 wt % and 12 wt %. Dry polyurethane films presented good mechanical properties, while hydrolytic degradation studies performed on PUs hydrogels showed that the polymers lost 10% of mass after 90 days in a simulated body fluid.

Based on previous studies,^{11,22,23} the aim of this work is to synthesize novel chemically crosslinked polyurethane hydrogels with thermo-responsive behavior and good mechanical properties. To achieve these objectives, the crosslinked polyurethane

hydrogels were synthesized in a one-shot route based on PEG and PCL-diol, as hydrophilic and hydrophobic segments, respectively, to induce thermosensitive behavior, biocompatibility, and biodegradability, HDI as isocyanate due to low toxicity, and PCL-triol as hydrolysable crosslinking agent. The total PCL amount (PCL-diol + PCL-triol) in the PU varied in the range from 11 wt % to 55 wt %. The precursors were previously characterized by hydroxyl index in order to ensure the reaction stoichiometry and to promote controlled and reproducible synthesis. Moreover, the average molar mass of the precursors is higher than those used elsewhere^{11,22} ($M_n \approx 2000$ – 3000 g/mol), aiming at improving the elasticity. The choice of HDI as diisocyanate was also based on the fact that it strongly affects the mechanical properties and crystallinity of the polyurethanes.¹³

EXPERIMENTAL

Materials

Poly(ethylene glycol) (PEG), poly(caprolactone) diol (PCL-diol), and poly(caprolactone) triol (PCL-triol) were purchased from Sigma Aldrich. PEG was vacuum dried at 60 °C for 48 h, and the other precursors were vacuum dried at 60 °C overnight before use. Dibutyltindilaurate (95%) and hexamethylene diisocyanate (HDI, 98%), purchased from Sigma Aldrich, were used as received. 1,2-Dichloroethane (99%) and ethanol (99.5%) were purchased from Synth, being dichloroethane distilled before use.

The hydroxyl indices of PEG, PCL-diol, and PCL-triol, expressed in terms of mol of hydroxyl groups per gram of homopolymer (mol OH/g), were determined using the method described by Kricheldorf and Meier-Haack.²⁵ Basically, this method consists of determining the molar ratio of the end groups and the total mers using proton nuclear magnetic resonance (¹H NMR) spectroscopy after a fast and stoichiometric reaction between trifluoroacetic anhydride and the hydroxyl end groups (–CRHOH) of the macrodiols. The emboldened hydrogen in the –CRH–OCOCF₃ end group is shifted from the typical signal of the mers, allowing the quantitative analysis. The hydroxyl index was also used to calculate the numerical average molar mass (M_n).

Gel permeation chromatography (GPC) was performed on a Viscotek GPCmax VE 2001 chromatograph equipped with a Viscotek VE3580 RI detector and Viscotek UV Detector 2500, Viscotek TGuard 10 × 4.6 mm guard column, and three Shodex KF-806M columns. The column system was kept at 40 °C. Anhydrous tetrahydrofuran (Tedia, HPLC grade) was used as eluent at a flow rate of 1.0 mL/min, as well to prepare polymer solutions of 8.0 mg/mL. Molar masses are relative to polystyrene (PS) standards (Viscotek) with molar masses from 1050 to 3,800,000 g/mol.

Synthesis of Chemically Crosslinked and Segmented Polyurethanes

Chemically crosslinked and segmented polyurethanes derived from PEG, PCL-diol, and PCL-triol were synthesized in a one-step route. Dry PEG, PCL-diol, and PCL-triol were added in the reaction flask together with 50 μL of the dibutyltindilaurate. The reaction mixtures were dried under a vacuum for 2 h. After

Table I. Reaction Medium and PU Compositions Obtained from the ^{13}C NMR Spectra

#	PU	Reaction medium (mass fraction %)				Soluble fraction (mass %)		Composition (mass %) ^b			
		PEG	PCL-diol	PCL-triol	PCL ^a	In water	In chloroform	After water extraction		After chloroform extraction	
								PEG	PCL ^a	PEG	PCL ^a
1	(89:0:11)	89	0	11	11	11 ± 1	21 ± 4	83	17	79	21
2	(79:0:21)	79	0	21	21	18 ± 1	26 ± 4	76	24	71	29
3	(67:22:11)	67	22	11	33	3.0 ± 0.1	33 ± 5	~67	~33	76	24
4	(45:44:11)	45	44	11	55	1.0 ± 0.1	53 ± 5	~45	~55	50	50

^aTotal PCL content.^bDetermined by ^{13}C NMR.

this, dry 1,2-dichloroethane was added and the reaction medium was purged with argon (99.999%) under stirring and heated up to 45 °C. HDI was added to the homogeneous solution at (NCO:OH) molar ratio of (1:1). After homogenization, the reaction was conducted at 45 °C without stirring for 48 h, and then it was finished by adding 1 mL of ethanol. The resulting organogel was allowed to swell in ethanol for another 2 h to ensure that all remaining isocyanate was consumed. The resulting organogel was dried at 60 °C for 24 h. The PEG:PCL-diol:PCL-triol mass fractions used to synthesize the polyurethanes are summarized in Table I.

The PU were subjected to a selective extraction using water in order to extract non-reacted PEG, catalyst, and other water-soluble products, or using chloroform in order to extract non-reacted PCL, PEG, and other CHCl_3 soluble materials. The extractions were performed by swelling the polymer with water or chloroform, replacing the solvents many times to ensure extraction efficiency. After extraction with water, a fraction of the hydrogels was characterized as well, while another fraction was dried under a vacuum at 60 °C for 48 h, and then analyzed. Samples subject to extraction with chloroform were also dried under the same conditions and then analyzed by ^{13}C NMR. The amount of soluble fractions was determined by gravimetry.

Characterization

Fourier transform infrared spectroscopy (FTIR) analyses of non-extracted PU were conducted on an Agilent Technologies Cary 630 FTIR equipment in the attenuated reflectance mode (ATR) in the range from 4000 to 400 cm^{-1} , resolution of 2 cm^{-1} , and 64 scans.

All the other characterizations were carried out with water extracted PU, except by those highlighted as “after extraction with chloroform”. The samples subjected to water extraction are named PUa.

The ^{13}C NMR analyses were performed on a Bruker Avance 500. Around 30 mg of the water or chloroform insoluble fraction of the polyurethanes were ground, dried, and placed in the amostral tube followed by addition of 1 mL of CDCl_3 . The spectrum of the swollen samples was acquired without the

nuclear Overhauser effect, with the equipment operating at 25 °C, 11.7 Tesla, pulse delay of 1 s, pulse interval of 60 s, number of scans equal to 3572, and free induction decay (FID) resolution of 0.5 Hz.

Differential scanning calorimetry (DSC) of the dry PUa was performed on a DSC Q2000, TA Instruments, according to the program: (1) heating from room temperature to 200 °C at 20 °C/min followed by 3 min isotherm; (2) cooling at -10 °C/min to -100 °C followed by 5 min isotherm; and (3) heating at 10 °C/min to 200 °C.

The X-ray diffraction (XRD) analyses of the PUa were conducted from 2° to 50° at the rate of 2°/min rate and tension of 40.0 kV on a SHIMADZU XRD-7000.

Water swelling measurements were conducted with PUa at different temperatures and in triplicate. Samples of dry PUa weighing around 50 mg were subjected to swelling in distilled water at constant temperature. After 24 h, time sufficient to achieve swelling equilibrium, the samples were removed from water, dried using a smooth paper, and weighed in an analytical balance (10^{-4} g precision). After weighting, the samples were subjected to swell in other temperatures.

Samples for scanning electron microscopy (SEM) were prepared according to the following procedure: first, PUa hydrogel samples were carefully sliced with a sharp blade; the sliced face was further subject to the analysis. The sliced samples were placed into distilled water and cooled to 4 °C, and then they were taken out of water and subjected to freezing at -10 °C. After this, the samples were cooled down in liquid nitrogen and subjected to freeze-drying in a Liotop K105 equipment for 24 h. After freeze-drying, the samples were fixed on the sample holder with a graphite tape, metalized with gold and palladium, and then analyzed on a JEOL JSM-6360LV equipment.

Thermoporosimetry of PUa hydrogels was conducted on a DSC Q2000, TA Instruments. The PUa hydrogels were surface dried with sorbent paper before being placed on a hermetic sample holder of aluminum and then analyzed according to the program: (1) Cooling to -30 °C at 1 °C/min rate, followed by 5 min of isotherm; and (2) heating to 30 °C at 1 °C/min rate.

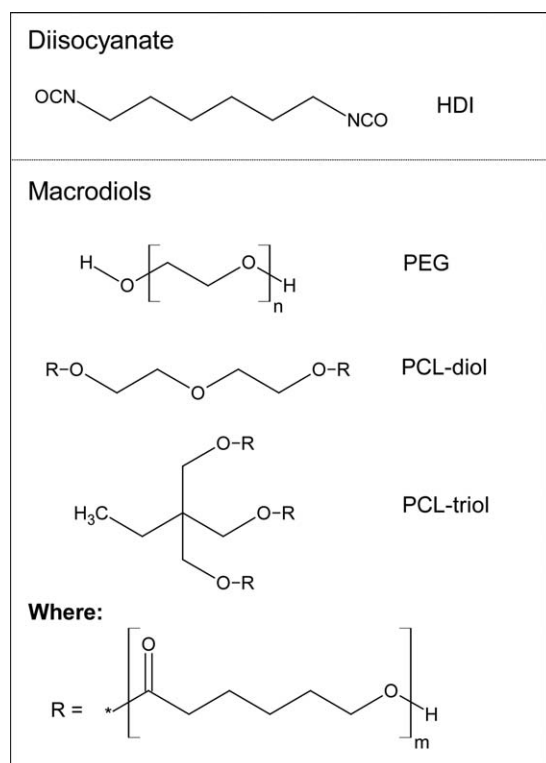


Figure 1. Molecular structures of diisocyanate and macrodiols.

Compression tests on the hydrogels were conducted on a TMA 2940 TA Instruments. Cylinders with 5 mm height and 6 mm diameter were subjected to a cycle of loading and unloading at 25 °C following the program: (1) loading of 0.05 N/min to 0.5 N and (2) unloading of 0.05 N/min to 0.0001 N.

RESULTS AND DISCUSSION

Figure 1 shows the molecular structure of the macrodiols and diisocyanate used to synthesize the polyurethanes. The average molar mass (M_n), polydispersity index (M_w/M_n), and the hydroxyl index of commercial PEG, PCL-diol, and PCL-triol macrodiols are shown in Table II.

The synthesis of polyurethanes from polyols and diisocyanates at temperatures higher than 60 °C may lead to byproducts (e.g. allophanate and biuret formation, etc.).^{5,26} While these products contribute to PU crosslinking, the network become more complex, with a variety of different chemical crosslinks. In this work, however, the reactions were conducted at 45 °C and a rigorous stoichiometry and humidity control were adopted. Under

Table II. Molar Mass and Hydroxyl Index of the Macrodiols

Macrodiol	M_n^a (kg/mol)	M_w/M_n^a	M_n^b (g/mol)	[OH] ^b (mmol/g)
PEG	3.0	1.03	2072	0.97
PCL-diol	2.3	1.86	2169	0.92
PCL-triol	1.3	1.48	727	4.1

^a Determined by GPC.

^b Determined by ¹H NMR.

these conditions, side reactions were avoided and the crosslinking density of the PU is controlled by the relative amount of PEG, PCL-diol, and PCL-triol. The adopted nomenclature for PU uses the structure PU(X:Y:Z) or PU(X:Y:Z)_a, where X, Y, and Z are, respectively, the mass percentages of PEG, PCL-diol, and PCL-triol used in the synthesis, and “a” denotes the PU after water extraction.

FTIR spectra of the polyurethanes are shown in Figure 2. The spectra present the main and characteristic bands of polyurethanes at 3300 cm^{-1} (N–H bond stretching), at 1700 cm^{-1} (C=O bond stretching), at 1600 cm^{-1} (related to the C–N bond stretching), and at the region between 900 and 1300 cm^{-1} (related to the C–O–C bond stretching). The bands related to the C–N and N–H stretching proved the formation of the urethane linkage, while the shoulders observed in the bands related to carbonyl and C–O–C stretching indicate that there are two different types of carbonyl and ester linkages, assigned to the polyester PCL segments, and to the urethane groups.

Chemically crosslinked PU are insoluble in any solvent. However, a fraction of the macrodiols did not react. The data of the water and chloroform soluble fraction of the PU are shown in Table I. While water extracts free PEG and its PEG richer polyurethane oligomers, chloroform extracts free PEG, PCL, and polyurethane oligomers. The water-soluble fraction is relatively insignificant for PU containing 45 wt % and 67 wt % of PEG (Table I, entries 3 and 4). However, it varies from (11 ± 1)% to (18 ± 1)% for PU containing 89 wt % and 79 wt % of PEG (Table I, entries 1 and 2), respectively. However, the chloroform soluble fraction is higher, reaching the value of 53 wt % for PU containing 45 wt % of PEG (Table I, entry 4). These results indicate that when dealing with binary systems of PEG and PCL-triol, PEG is the major component in the soluble fraction, suggesting that the hydroxyl end groups of low molar mass PCL-triol are more accessible or reactive to the isocyanates. In ternary systems composed of PEG, PCL-diol, and PCL-triol, PCL is the major component in the soluble fraction, suggesting

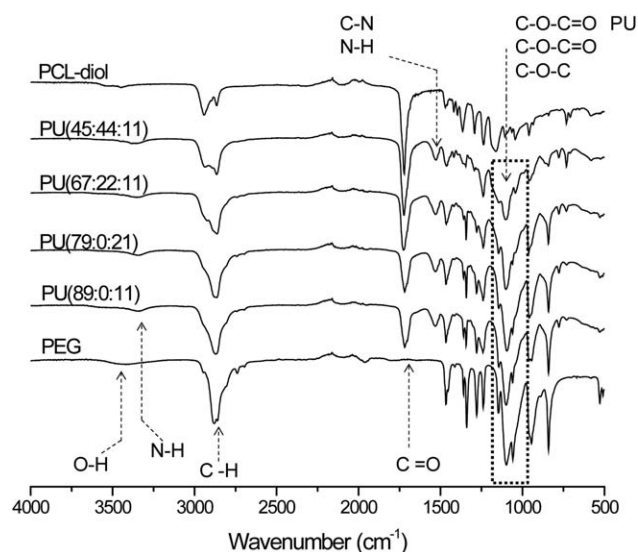


Figure 2. FTIR spectra of the polyurethanes.

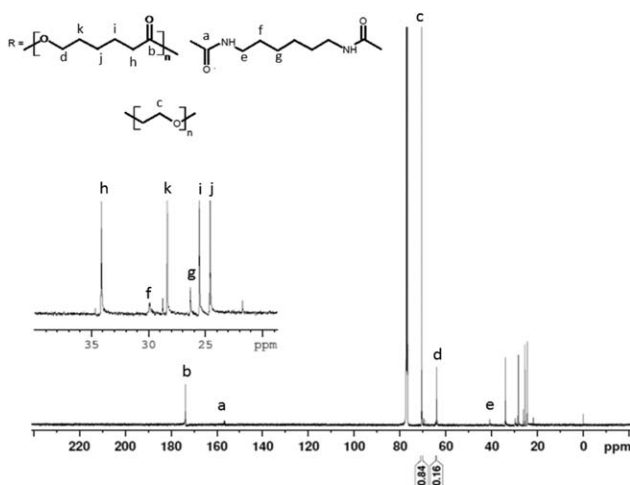


Figure 3. ^{13}C NMR spectrum for PU(45:44:11) after extraction with chloroform.

a lower reactivity of hydroxyl groups of PCL-diol compared to PEG hydroxyl groups.

The compositions of PU subjected to water and chloroform extractions were determined by ^{13}C NMR, Table I. The ^{13}C NMR spectrum of PU(45:44:11) after extraction with chloroform is shown in Figure 3. The spectra for the other PU subjected to water or chloroform extractions can be found in the Supporting Information (Supporting Information, Figures S1–S5). In this spectrum, the following signals are observed: $-\text{CH}_2\text{-PEG}$ units at 71 ppm, $\text{C}_b, \text{C}_d, \text{C}_h, \text{C}_i, \text{C}_j,$ and C_k of PCL units at 173, 62, 34, 25.4, 24.5, and 28.5 ppm, respectively, and $\text{C}_e, \text{C}_f,$ and C_g (at 40, 30, and 26 ppm, respectively) corresponding to HDI segments, as well as signals corresponding to the carbamide group (C_a , at 156.7 ppm).¹⁹ The PU compositions, determined from the area ratio of the signals corresponding to PEG and PCL chains (C_c and C_d , Figure 3), are expressed in terms of the mass percentage of PEG and total PCL (Table I).

The extraction experiments were very useful to elucidate the network structure of PU. Table I shows that the composition after water extraction is close to the reaction medium for the ternary polyurethanes based on PEG, PCL-diol, and PCL-triol.

However, the binary PU (based only in PEG and PCL-triol) presents a lower PEG amount than was planned. Moreover, the ternary hydrogels resulting from water swelling of PU after water extraction contain a fraction of unreacted PCL and possibly linear PCL polyurethane oligomers.

Considering the results from the extraction assay, all the PUs were subjected to water extraction before the subsequent characterization as PUa and as the corresponding hydrogels.

DSC curves for dry PUa are shown in Figure 4. The melting temperature, melting enthalpy and glass transition temperature (T_m , ΔH_m , and T_g , respectively, taken from second heating DSC curves) as well as crystallization temperature (T_c , taken from cooling DSC curves) are shown in Table III. The macrodiols present similar molar masses (Table II) and they are semicrystalline (Table III). The second heating scan curves [Figure 4(c)] show a glass transition region below 0°C and melting region above 30°C . The T_g and T_m values for PEG are -48°C and 55°C , respectively. For PCL, T_g is -65°C and two melting peaks are observed at 39°C and 45°C , due to a recrystallization (Figure 4). Only a single glass transition is observed in the second heating scan for PUa. Depending on the composition, the glass transition is shifted to a higher temperature compared to T_g of PEG or PCL. This shift results from the contributions of the urethane hard segments and also from restrictions imposed by the crosslinked structure, which reduce the free volume of the amorphous phase and chain flexibility.^{27,28} Also, the presence of a unique glass transition [see the zoomed-in-view of the glass transition region, Figure 4(c)] suggests the miscibility of PEG and PCL in the amorphous phase. The PEG/PCL and poly(ethylene oxide) (PEO)/PCL miscibility are controversial. According to Qiu *et al.*,²⁹ PCL ($M_w = 14,300$ g/mol) and PEO ($M_w = 100,000$ g/mol) are immiscible. However, Chang and coworkers³⁰ reported miscibility for PCL ($M_w = 56,000$ g/mol) and PEO ($M_w = 100,000$ g/mol). Li *et al.*³¹ determined the phase diagram of PCL/PEO blends ($M_w = 20,000$ g/mol for both polymers) and found a miscibility window associated to upper critical solution temperature (UCST) behavior. Nojima *et al.*³² reported that the crystallization of both polymers in PEG/PCL blends occurs into the respective polymer domains, meaning the blends are immiscible. On the contrary, for poly(ethylene

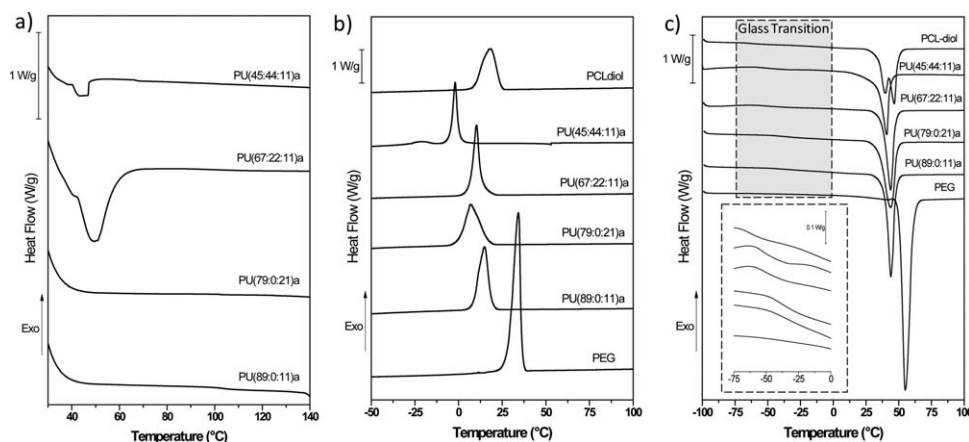


Figure 4. DSC curves for dry PUa: (a) first heating, (b) cooling, and (c) second heating.

Table III. Thermal Properties Obtained from the DSC Second Heating Scan for the Precursors and PUa

		T_c (°C)	T_g (°C)	T_m (°C)	ΔH_m (J/g)	Q (%) 25 °C	Young's modulus (Pa)
1	PEG	38	-48	55	174	-	-
2	PU(89:0:11)	22	-30	43	82	575 ± 16	4300 ± 50
3	PU(79:0:21)	21	-40	43	81	385 ± 10	10,100 ± 100
4	PU(67:22:11)	21	-52	44	71	250 ± 10	7460 ± 107
5	PU(45:44:11)	3	-53	40	63	115 ± 5	22,870 ± 180
6	PCL-diol	27	-65	39 (46) ^a	74	-	-

^aRecrystallization followed by a second melting event was observed.

glycol)-poly(ϵ -caprolactone) block copolymers, the crystals of both blocks are formed in the same PLC-PEG domain and because of this, both blocks crystallize under mutual influence.

Cooling curves [Figure 4(b)] reveal exothermic peaks centered at 34 °C and 18 °C for PEG and PCL-diol, respectively. All PU present one peak in the temperature range from -10 °C to 20 °C, with the exception of PU(45:33:11)a, for which a main peak is observed around -2 °C and another one with lower intensity is observed around -20 °C. The second heating scans [Figure 4(c)] show endothermic peaks at temperatures intermediate to the melting temperature of PEG and PCL-diol. For PU(89:0:11)a and PU(79:0:21)a, in which PCL-diol is absent, the crystalline phase is due to PEG. The decrease of T_m of these PUa compared to neat PEG (Table III) is due to the decrease of the crystallization temperature, and therefore the decrease of lamellae thickness, induced by crosslinking.

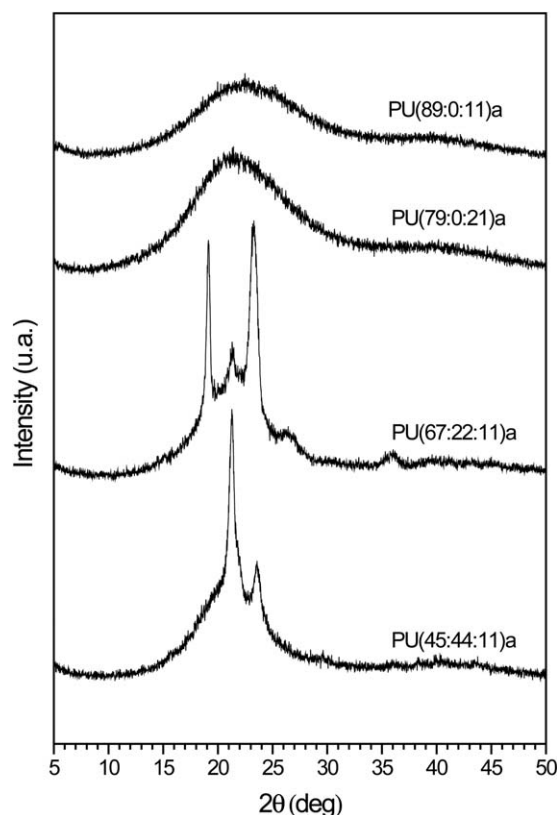
While the PUs synthesized in this work are able to crystallize, similar polyurethanes reported by Barrioni *et al.*,¹¹ based on low mass PEG, glycerol, HDI, and PCL-triol, are amorphous, probably as a consequence of the small length of the PEG and PCL segments in the network. The influence of the macrodiols molar mass on the PU crystallinity was also verified by París *et al.*²³ These authors showed that chemically crosslinked polyurethanes composed of low molar mass PEG, PCL-diol, PEG-triol, PEG-tetraol, and HDI are amorphous when PEG 600 (600 g/mol) was used; however, it is semicrystalline when 10% of the PEG 600 was replaced with PEG 1500 (1500 g/mol).

The first DSC heating scans [Figure 4(a)] present a melting peak only for PU(45:44:11)a and PU(67:22:11)a. The X-ray diffractograms shown in Figure 5 corroborate this result. The diffractogram for PU(67:22:11)a presents peaks assigned to the crystalline phase of the PEG ($2\theta = 19^\circ$ and 23°) and of the PCL ($2\theta = 21^\circ$ and 24°), while for PU(45:44:11)a the diffractogram presents only peaks relative to the crystalline patterns of PCL,^{32,33} in this case, PEG crystallization was suppressed.

According to DSC and X-ray diffractometric data, the PUa subjected to water swelling present different characteristics: PU(89:0:11)a and PU(79:0:21)a are amorphous, while the other PUa are semicrystalline. Besides the global composition differences, the presence of a crystalline phase and of free PCL-diol chains should have an impact on the water swelling capacity and on the mechanical properties of the hydrogels. The crystal-

line phase contributes to increase the crosslinking density, since they act as a physical crosslinker.

Water uptake capability [$Q = (m - m_i)/m_i \times 100$, where m and m_i are the mass of the swollen and dry samples, respectively] was evaluated as a function of the temperature. Water uptake depends on the composition and on the crosslinking density (Figure 6). Both parameters determine the water swelling equilibrium. While the difference of the chemical potential of the solvent in the swollen polymer and neat solvent is the drive force to the swelling, the crosslinking density determines the elastic force of the network and therefore, its resistance to swell.³⁴ The difference in water uptake of the binary PU(89:0:11)a and PU(79:0:21)a is related to the increase in the crosslinking density. This property for the ternary PUa depends also on the PCL contents, which is a hydrophobic and semicrystalline component, both factors contribute to decrease the water

**Figure 5.** X-ray diffractograms for PUa.

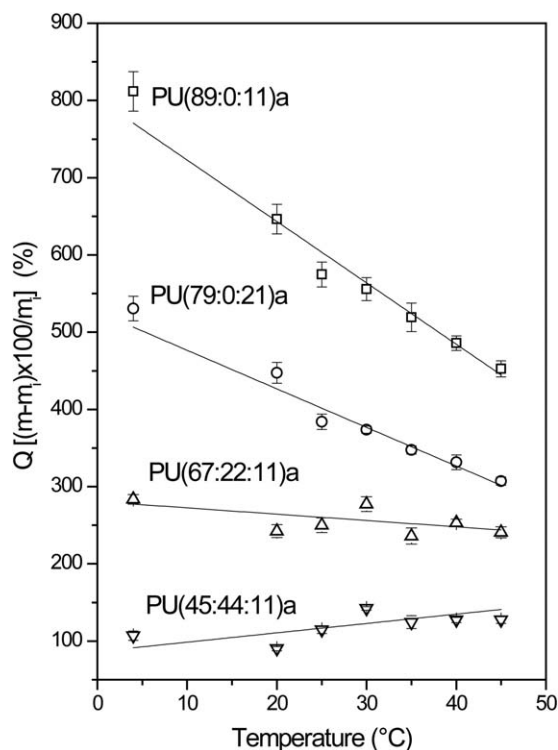


Figure 6. Water uptake for the PUa at equilibrium at different temperatures.

swelling capacity. In general, the increase of the temperature resulted in a continuous and monotonic reduction of the water uptake for PEG-rich PUa. Paris *et al.* also related a negative dependence of the water uptake with increasing temperature for PEG rich polyurethanes.²³ This behavior indicates that PUa/water systems present a typical lower critical solution temperature (LCST), although no sharp transition is observed. The LCST behavior is governed by hydrogen bonding between water and polymer, and by the hydrophobic interactions between non-polar segments of the polymer network.² It is noteworthy that the increase of PCL content in the hydrogels leads to a gradual change of a negative swelling behavior to a positive one. For PUs containing high amount of PCL, PU(45:44:11), a tendency of the increase of water uptake with increasing temperature is observed. There are few reports in the literature about polymer/water systems that present an upper critical solution temperature (UCST).³⁵ In this case, the interactions between PCL segments could be responsible for this effect. These interactions could act as physical crosslinking, whose density decreases with increasing temperature, increasing the swelling capacity.

For all the PUa, the temperature dependence of the water uptake is continuous in the studied temperature range (4 °C to 45 °C), with no abrupt decays (characteristic of the critical temperature phenomenon). The variation of the water uptake capability of the PU(89:0:11) when changing the temperature from 20 °C to 40 °C ($\Delta T = 20$ °C) is 158%, which allows a controlled liberation of sorbed materials from the matrix, such as drugs or other substances.⁸ The Q values at 25 °C, summarized in Table

III, vary from 115% to 575% when PEG content varies from 45 wt % to 89 wt %.

The hydrogels collapsed after lyophilization and heating up to room temperature. As a consequence, SEM images show a folded structure (Figure 7). This collapse occurs because the glass transition of the PUa is below room temperature and the presence of a crystalline phase is not enough to ensure dimensional stability of the porous walls. The images of the collapsed PUs reveal a similar structure for PU(89:0:11)a and PU(79:0:21)a: small pores uniformly distributed through the material surface and with comparable diameter [Figure 7(a,b)]. While PU(67:22:11)a presents also a porous morphology, these pores are larger and their number is smaller [Figure 7(c)]. PU(45:44:11)a seems to be more dense and the porous structure is not defined [Figure 7(d)]. The porosity of the lyophilized hydrogels is directly related to the composition; more specifically, to the PEG content and to the PUa water uptake capacity. PEG rich networks are capable of forming small and numerous pores, increasing the interfacial area between polymer chains and water. On the other hand, for PCL rich networks, the large and sparse pores minimize the polymer–water interface. The order of apparent porous diameter is [PU(89:0:11)a \approx PU(79:0:21)a] < PUTR(67:22:11)a < PU(45:44:11)a.

PU hydrogels were also subjected to a thermo-porosimetry using DSC. Thermo-porosimetry consists of determining the water crystallization temperature into the hydrogel.³⁶ The crystallization temperature of water present in the pores decreases as the pore diameter decreases in consequence of the intermolecular interactions between water and the polymer chains, and due to capillarity effect.³⁵ Cooling DSC curves for the hydrogels and the crystallization temperature of sorbed water as a function of the PEG content are shown in Figure 8. The crystallization temperatures were taken as the onset. The loop observed after the start of the crystallization is an artifact related to the extremely exothermic crystallization of the water, releasing a large amount of energy, which overcomes the equipment capacity for temperature maintenance.³⁷

In general, the increase in the PEG amount in the hydrogels leads to a reduction of the crystallization temperature, indicating a decrease in pore size, which corroborates the SEM results. An exception is verified for the sample PU(45:44:11), probably due to its considerably lower water uptake capacity and consequent formation of smaller pores in which the water is located (Figure 6). According to these results, the proposed order of increasing pores size is: PU(89:0:11)a \sim PU(79:0:21)a \sim PU(45:44:11)a < PU(67:22:11)a.

The heating DSC curves in Figure 8(c), allows us to verify that water is present in three different environments into the hydrogels: bounded water, bulk water, and free water.³⁵ Bounded water is present in the interface between water and the polymeric matrix, and presents the lowest melting temperature (around -18 °C). Bulk water is located in the inner pores, however is still influenced by the interfacial tension, and melts at approximately 0 °C for the PUa. Free water is present inside larger pores and its melting temperature is around 3 °C, a temperature that is close to the melting of neat water. The water

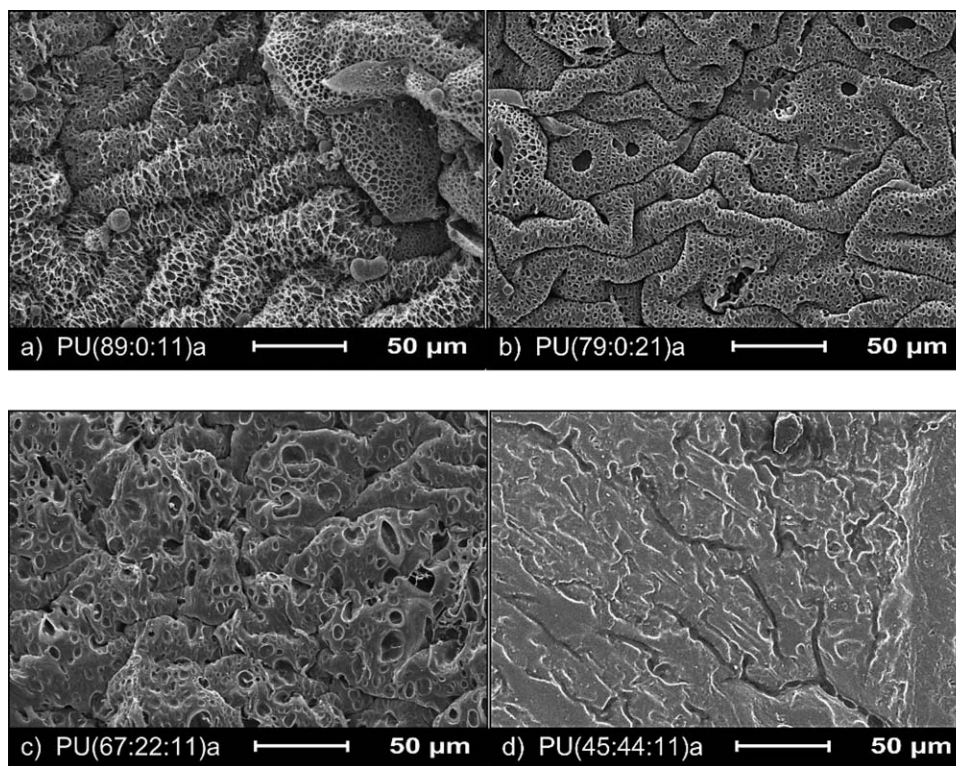


Figure 7. SEM micrographs obtained for PUa (a) PU(89:0:11)a, (b) PU(79:0:21)a, (c) PU(67:22:11)a, and (d) PU(45:44:11)a.

into PU(45:44:11)a did not present the melting event around -18°C because the amount of bounded water is probably too low to be detected, due to the hydrophobicity of the polymer network caused by the high PCL content.

The mechanical properties of the hydrogels were evaluated by unconfined compression tests performed at 25°C . Hydrogels were subjected to a loading and unloading compression cycle at a constant tension rate. The experimental arrangement and the loading/unloading program are shown in Figure 9(a,b), respectively.

All hydrogels are elastic under compression and return almost to their original dimensions when the compressive tension is

released, as can be seen in Figure 9(c). The observed hysteresis is associated with the permanent deformation of the samples, while the area within the loading and unloading curves is proportional to the dissipated mechanical energy per cycle and to hydrogel toughness.³⁸ For an elastic matrix, full recovery of the energy is expected (i.e., no hysteresis) meaning that PUa hydrogels present a viscoelastic behavior. Moreover, Figure 9(c) shows that the increase of PEG contents in the PUa, which results in an increase of water content in the hydrogel, leads to an increase of the toughness. The Young's Modulus of the hydrogels (Table III), calculated as the slope of the initial part of the loading curves, increases in the following order: PU(89:0:11)a < PU(67:22:11)a < PU(79:0:21)a < PU(45:44:11)a.

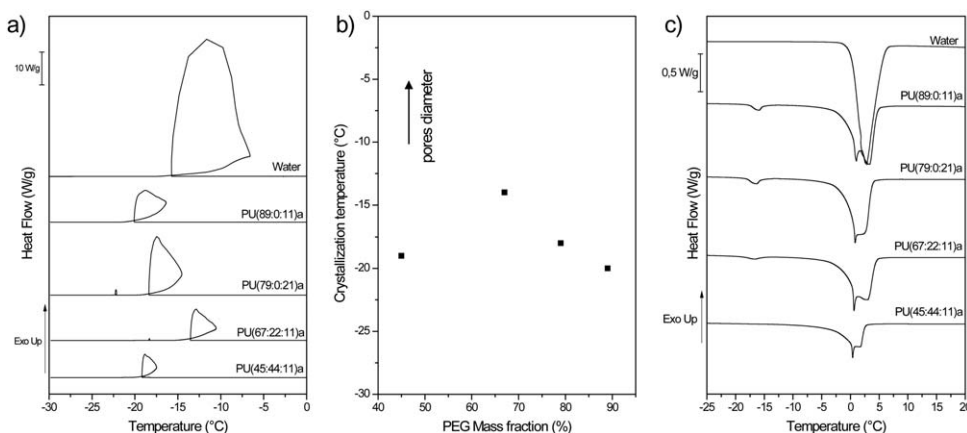


Figure 8. Thermo-porosimetry analysis for the PUa hydrogels: (a) Cooling DSC curves; (b) Crystallization temperature of sorbed water as a function of the hydrogel composition; and (c) heating DSC curves.

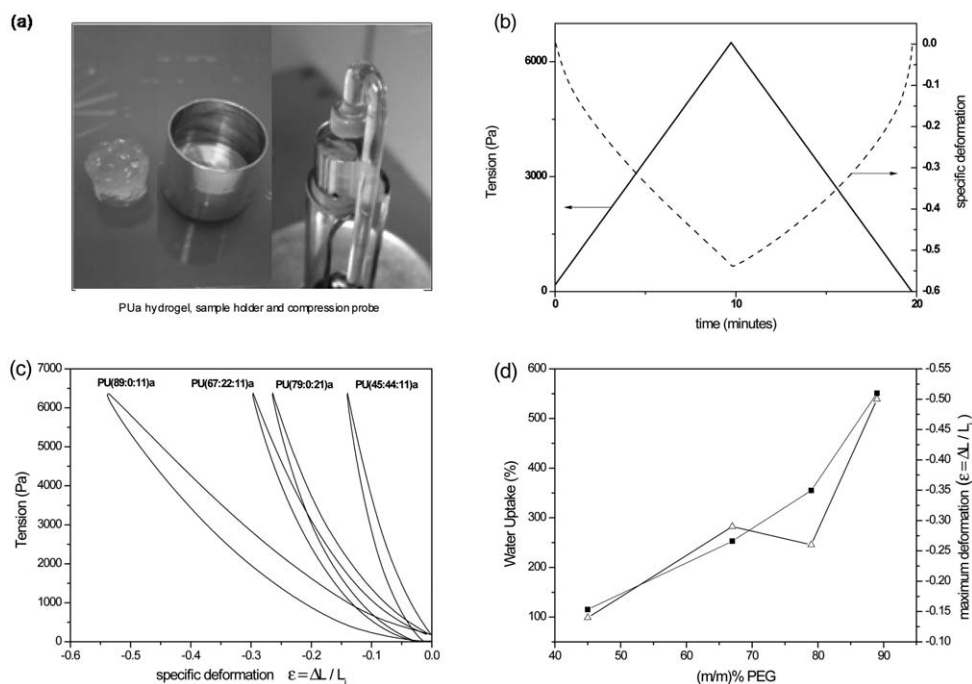


Figure 9. (a) Pictures of PUa hydrogel, sample holder and compression probe, (b) loading/unloading ramp and specific deformation for PU(89:0:11)a, (c) tension vs. deformation curves from unconfined compression tests, and (d) water uptake (■) and maximum deformation at 6500 Pa tension (△) as a function of the composition and at 25 °C.

The maximum deformation at 6500 Pa presents an opposite trend. The increase in the PCL diol or in the PCL-triol results in an increase of the Young's modulus due to the increase of the physical and chemical crosslinking density, respectively. For binary PUa, the increase in crosslinking density led to an increase in the modulus, as observed for PU(89:0:11)a and PU(79:0:21)a (4 kPa and 10 kPa, respectively). Comparing PU(67:22:11)a and PU(45:44:11)a hydrogels, which were prepared using the same amount of PCL triol (i.e., 11 wt %), the increase of PCL diol from 22 to 44 wt % led to an increase in the modulus from 7 kPa to 23 kPa (Table III) due to the presence of a crystalline phase. However, for comparison of the PU(67:22:11)a and PU(79:0:21)a hydrogels, some peculiarities should be taken into account. The composition of the networks after extraction with chloroform, meaning the composition of the networks without free macrodiol (PEG or PCL) chains and polyurethane oligomers, is close for these two PUa: PEG/PCL_{total} mass fraction equal to 71 : 29 and 76 : 24 for PU(79:0:21)a and PU(67:22:11)a, respectively. On the other hand, the composition of hydrogels (with water extracted PU) also expressed as PEG/PCL_{total} mass fraction is 76:24 and 67:33 for PU(79:0:21)a and PU(67:22:11)a, respectively. As previously discussed, the PU(67:22:11)a hydrogel contains PCL free chains and probably polyurethane oligomers. Moreover, the amount of the PCL triol crosslinker is higher in the PU(79:0:21)a. Therefore, the water uptake capacity of these PUa and the mechanical properties of the corresponding hydrogels are determined by both factors: crosslinking density and PCL amount. Figure 9(d) shows the water uptake capacity and the maximum deformation achieved for each hydrogel at 6500 Pa as a function of the PU composition, expressed as mass fraction of the PEG. The water uptake

capacity seems to be more influenced by the total PCL amount in these hydrogels than the crosslinking density ($Q = 385\%$ and 115% for PU(79:0:21)a and PU(67:22:11)a at 25 °C, respectively). On the contrary, the Young's modulus (E) and the maximum deformation (ϵ) at 6500 Pa tension seems to be more influenced by the crosslinking density than the PCL content [$E = 10$ kPa and $\epsilon = 0.26$, and $E = 7$ kPa and $\epsilon = 0.29$ for PU(79:0:21)a and PU(67:22:11)a at 25 °C, respectively].

CONCLUSIONS

Chemically crosslinked polyurethanes based on PEG and PCL macrodiols were successfully synthesized in a single step reaction. While water and chloroform extraction indicated the presence of a soluble fraction constituted by residual precursors and possibly polyurethane oligomers, all PU presented an insoluble crosslinked matrix. The water sorption capacity of the polyurethanes is related to the PEG content, reaching up to 600% at room temperature for PEG rich materials. In addition, the PEG rich hydrogels presented a negative dependence of the water uptake with the increase of the temperature, while the increase of PCL content in the PUa results in a gradual decrease of the slope of the Q vs. T curves, becoming slightly positive for PCL richer PUa. The water in the hydrogels is present in different environments as bounded, bulk, and free water. Water swelling induces a porous structure for PUa, whose morphological characteristics are determined by PUa composition. Under unconfined compression, the hydrogels showed low hysteresis and good dimensional recovery, a characteristic behavior of viscoelastic materials. The mechanical properties of the hydrogels are predominantly determined by the water content and, therefore, by the PEG content in the PUa. The architecture and chain

length between crosslinking bonds confers different thermal properties compared to other similar polyurethane hydrogels based on PEG and PCL: all the PU are able to crystallize, while PU based in low mass PEG and PCL are essentially amorphous.^{11,23}

ACKNOWLEDGMENTS

The authors acknowledge FAPESP–Brazil (Processes n° 2010/17804-7 and 2011/09479-1), CNPq–Brazil (Processes n° 444392/2014-9 and 150664/2015-0), and SAE-UNICAMP for the financial support.

REFERENCES

1. Ullah, F.; Othman, M. B. H.; Javed, F.; Ahmad, Z.; Akil, H. *Mat. Sci. Eng. C* **2015**, *57*, 414. DOI: 10.1016/j.msec.2015.07.053
2. Buenger, D.; Topuz, F.; Groll, J. *Prog. Polym. Sci.* **2012**, *37*, 1678. DOI: 10.1016/j.progpolymsci.2012.09.001
3. Cherg, J. Y.; Hou, T. Y.; Shih, F. M.; Talsma, H.; Hennink, W. E. *Int. J. Pharm.* **2013**, *450*, 145. DOI: 10.1016/j.ijpharm.2013.04.063
4. Hafeman, A. E.; Li, B.; Yoshii, T.; Zienkiewicz, K.; Davidson, J. M.; Guelcher, S. A. *Pharm. Res.* **2008**, *25*, 2387. DOI: 10.1007/s11095-008-9618-z
5. Król, P. *Prog. Mat. Sci.* **2007**, *52*, 915. DOI: 10.1016/j.pmatsci.2006.11.001
6. Hafeman, A. E.; Zienkiewicz, K. J.; Carney, E.; Litzner, B.; Stratton, C.; Wenke, J. C.; Guelcher, S. A. *J. Biomater. Sci. Polym.* **2010**, *21*, 95.
7. Cometa, S.; Bartolozzi, I.; Corti, A.; Chiellini, F.; Giglio, D.; Chiellini, E. E. *Polym. Degrad. Stabil.* **2010**, *95*, 2013.
8. Dayananda, K.; He, C.; Park, D. K.; Park, T. G.; Lee, D. S. *Polymer* **2008**, *49*, 4968. DOI: 10.1016/j.polymer.2008.09.033
9. Lefebvre, F.; David, C.; Vander, W. C. *Polym. Degrad. Stabil.* **1994**, *45*, 347.
10. Huang, M. H.; Li, S.; Hutmacher, D. W.; Schantz, J. T.; Vacanti, C. A.; Baud, C.; Vert, M. *J. Biomed. Mater. Res.* **2004**, *69A*, 417. DOI: 10.1002/jbm.a.30008
11. Barrioni, B. R.; Carvalho, S. M.; Oréface, R. L.; Oliveira, A. A. R.; Pereira, M. M. *Mat. Sci. Eng. C* **2015**, *52*, 22. DOI: 10.1016/j.msec.2015.03.027
12. Loh, X. J.; Sng, K. B. C.; Li, J. *Biomaterials* **2008**, *29*, 3185. DOI: 10.1016/j.biomaterials.2008.04.015
13. Trinca, R. B.; Felisberti, M. I. *Int. Polym.* **2015**, *64*, 1326. DOI: 10.1002/pi.4920
14. Skarja, G. A.; Woodhouse, K. A. *J. Biomater. Sci. Polym. Edn.* **1998**, *9*, 271. DOI: 10.1163/156856298X00659
15. Cauich-Rodríguez, J. V.; Chan-Chan, L. H.; Hernandez-Sánchez, F.; Cervantes-Uc, J. M. In *Advances in Biomaterials Science and Biomedical Applications*; Pignatello, R., Ed.; Rijeka, Croatia, 2013. ISBN: 978-953-51-1051-4; InTech. DOI: 10.5772/53681. Available from: <http://www.intechopen.com/books/advances-in-biomaterials-science-and-biomedical-applications/degradation-of-polyurethanes-for-cardiovascular-applications> (accessed on December 08, 2015).
16. Lee, S. J.; Lee, S. K.; Kim, B. K. *J. Macromol. Sci.* **2014**, *53*, 254.
17. Lin, X.; Tang, D.; Yu, Z.; Feng, Q. *J. Mater. Chem. B* **2014**, *2*, 651.
18. Ding, M.; Li, J.; Tan, H.; Fu, Q. *Soft Matter* **2012**, *8*, 5414.
19. Li, Z.; Zhang, Z.; Liu, K. L.; Ni, X.; Li, J. *Biomacromolecules* **2012**, *13*, 3977.
20. Knop, K.; Hoogenboom, R.; Fischer, D.; Schubert, U. S. *Angew. Chem. Int.* **2010**, *49*, 6288.
21. Tan, J. P. K.; Kim, S. H.; Nederberg, F.; Fukushima, K.; Coady, D. J.; Nelson, A.; Yang, Y. Y.; Hedrick, J. L. *Macromol. Rapid Commun.* **2010**, *31*, 1187.
22. Sardon, H.; Tan, J. P. K.; Chan, J. M. W.; Mantione, D.; Mecerreyes, D.; Hedrick, J. L.; Yang, Y. Y. *Macromol. Rapid Commun.* **2015**, *36*, 1761.
23. Paris, R.; Fernández, Á. M.; Garrido, I. Q. *Polym. Adv. Technol.* **2013**, *24*, 1062.
24. Liu, Z.; Wu, X.; Yang, X.; Liu, D.; Jun, C.; Sun, R.; Liu, X.; Li, F. *Biomacromolecules* **2005**, *6*, 1713.
25. Kricheldorf, H. R.; Meier-Haack, J. *Makromol. Chem.* **1993**, *194*, 715.
26. Herrington, R.; Nafziger, L.; Hock, K.; Moore, R.; Casati, F.; Lidy, W. In *Flexible Polyurethanes Foams*, 2nd Ed.; Herrington, R., Hock, K., Eds.; The Dow Chemical Company: Midland, **1997**.
27. Mahanta, N.; Teow, Y.; Valiyaveetil, S. *Biomater. Sci.* **2013**, *1*, 519.
28. Rämö, V.; Anghelescu-Hakala, A.; Nurmi, L.; Mehtiö, T.; Salomäki, E.; Härkönen, M.; Harlin, A. *Eur. Polym. J.* **2012**, *48*, 1495.
29. Qiu, Z.; Ikehara, T.; Nishi, T. *Polymer* **2003**, *44*, 3101.
30. Chiu, C. Y.; Chen, H. W.; Kuo, S. W.; Huang, C. F.; Chang, F. C. *Macromolecules* **2004**, *37*, 8424.
31. Li, J.; Zhang, Y.; Jiaco, Y.; Shang, Y.; Huo, H.; Jiang, S. *Polym. Bull.* **2012**, *68*, 1405.
32. Nojima, S.; Ono, M.; Ashida, T. *Polym. J.* **1992**, *24*, 1271.
33. Sun, J.; He, C.; Zhuang, X.; Jing, X.; Chen, X. *J. Polym. Res.* **2011**, *18*, 2161.
34. Flory, P. J. *Principles of Polymer Chemistry*; Cornell University Press: Ithaca: **1986**.
35. Strandman, S.; Zhu, X. X. *Prog. Polym. Sci.* **2015**, *42*, 154.
36. Ishikiriyama, K.; Todoki, M. *J. Colloid Interf. Sci.* **1995**, *171*, 92.
37. Aubuchon, S. R. Interpretation of the Crystallization Peak of Supercooled Liquids Using Tzero[®] DSC. TA Instruments documentation. Available from: http://www.tainstruments.co.jp/application/pdf/Thermal_Library/Applications_Briefs/TA344.PDF (accessed on December 08, 2015).
38. Akhilesh, K. G.; Sandhya, A. D.; Jamie, M. C.; Chia-Jung, W.; Gudrun, S. *Biomacromolecules* **2011**, *12*, 1641.